

Manuscript Number: IJP-D-15-00286R1

Title: Controlled drug release from hydrogel-based matrices: experiments and modeling

Article Type: Research Paper

Section/Category: Pharmaceutical Nanotechnology

Keywords: Hydrogels, Water uptake, Texture analysis, Transport phenomena, Modeling.

Corresponding Author: Prof. Gaetano Lamberti, PhD

Corresponding Author's Institution: University of Salerno

First Author: Diego Caccavo

Order of Authors: Diego Caccavo; Sara Cascone; Gaetano Lamberti, PhD; Anna Angela Barba

Abstract: Controlled release by oral administration is mainly achieved by pharmaceuticals based on hydrogels. Once swallowed, a matrix made of hydrogels experiences water up-take, swelling, drug dissolution and diffusion, polymer erosion. The detailed understanding and quantification of such a complex behavior is a mandatory prerequisite to the design of novel pharmaceuticals for controlled oral delivery. In this work, the behavior of hydrogel-based matrices has been investigated by means of several experimental techniques previously pointed out (gravimetric, and based on texture analysis); and then all the observed features were mathematically described using a physical model, defined and recently improved by our research group (based on balance equations, rate equations and swelling predictions). The agreement between the huge set of experimental data and the detailed calculations by the model is good, confirming the validity of both the experimental and the theoretical approaches.

Dear Editor,

enclosed please find the revised version of the manuscript entitled **“Controlled drug release from hydrogel-based matrices: experiments and modeling”** (IJP-D-15-00286) by Diego Caccavo, Sara Cascone, Anna Angela Barba, and myself.

First of all I want to thank you and the reviewer for the work done, and for the nice comments. We went through the manuscript and we made the change the reviewer asked for. The new text is in red in the present version. Furthermore, in the next page you can find the list of the reviewer’s comments along with our answers, in red.

Look forward to hear from you

Fisciano (SA), 21st March 2015

Best Regards,

Gaetano Lamberti

Gaetano Lamberti

IJP AUTHOR CHECKLIST

Dear Author,

It frequently happens that on receipt of an article for publication, we find that certain elements of the manuscript, or related information, is missing. This is regrettable of course since it means there will be a delay in processing the article while we obtain the missing details.

In order to avoid such delays in the publication of your article, if accepted, could you please run through the list of items below and make sure you have completed the items.

Overall Manuscript Details

- Is this the final revised version?
- Are all text pages present?
- Are the corresponding author's postal address, telephone and fax numbers complete on the manuscript?
- **Have you provided the corresponding author's e-mail address?**
- **Manuscript type – please check one of the following:**
 - Full-length article
 - Review article
 - Rapid Communication
 - Note
 - Letter to the Editor
 - Other
- **Manuscript section – paper to be published in:**
 - Pharmaceutical Nanotechnology section
 - Personalised Medicine section

Manuscript elements

- Short summary/abstract enclosed?
- 3-6 Keywords enclosed?
- Complete reference list enclosed?
- Is the reference list in the correct journal style?
- Are all references cited in the text present in the reference list?
- Are all **original** figures cited in the text enclosed?
 - Electronic artwork format? -----
- Are figure legends supplied?
- Are all figures numbered and orientation provided?
- Are any figures to be printed in colour?
 - If yes, please list which figures here:-----
- If applicable, are you prepared to pay for reproduction in colour?
- Are all tables cited in the text supplied?

General

- Can you accept pdf proofs sent via e-mail?

Reviewers' comments:

Reviewer #1: This paper, dealing with the experimental and the modelling analysis of drug release from HPMC tablets, is well written and very interesting. Accordingly, its reading led to the following minor comments. In details:

1) Page 6, lines 176 - 177.

I would re-phrase this sentence as follows: From this pictures, both the swollen gel layer and the glassy core are clearly visible.

Done.

2) Page 6, lines 178 - 179.

This sentence is not clear. I suppose that the word "withdrawn" ha to be replaced by "withdrawing".

The reviewer was right, we changed the word.

3) Page 6, line 192.

The authors used HPLC to measure theophylline concentration. Is there any particular reason for using HPLC instead of the simpler and faster UV measurement?

It was a matter of convenience. We added a sentence at the end of page 6 to explain why: <<The large number of samples to be assayed has led to choose the use of HPLC over the faster UV-Vis method because of the availability of the automatized auto-sampler, which allowed to run a large number of testing overnight.>>

4) Page 7, eq.(1).

I do not understand why the matter flux depends also on the gradient of the average molar mass. Please explain.

The reason of this new terms have been explained in our previous work (Caccavo et al., 2015). However, a short sentence has been added on page 7, below Eq. 1: <<In particular, in the mass fluxes the Fick's first law for dilute systems, where the driving force is the molar fraction, has been translated for concentrate systems, where the driving force is the mass fraction. In this derivation the molar mass terms arise (Caccavo et al., 2015).>>

5) Page 7, eq.(4).

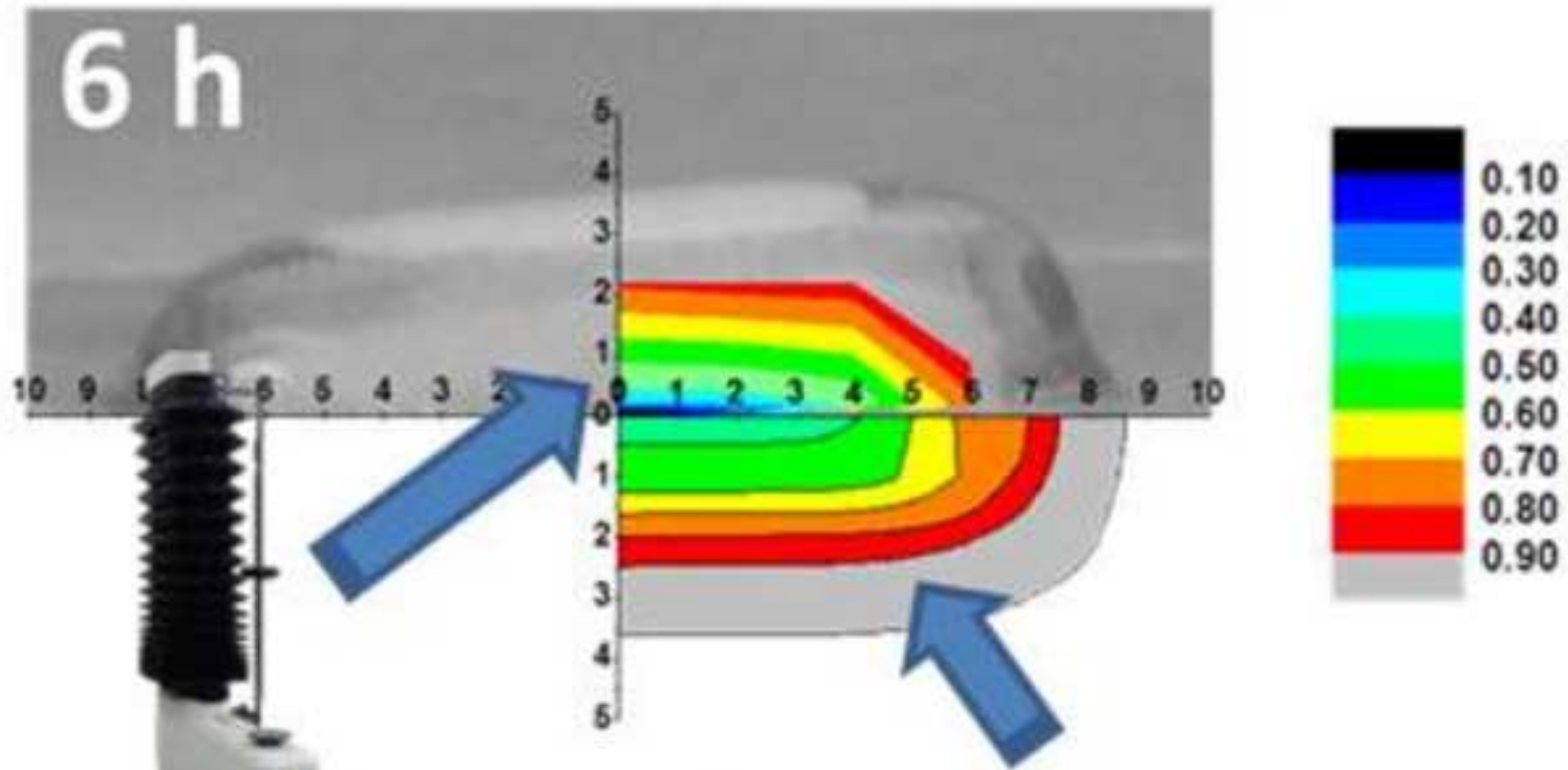
Which is the physical meaning of these equations? Which constraints do they impose to the matrix shape upon swelling?

Also these equations have been explained in our previous work (Caccavo et al., 2015). However, the text before and after Eq. 4 have been changed (extended) in order to give a better description of the physical meaning of that equations.

6) Page 7, line 251

I would replace "passes" by "elaps".

Done. (Actually, the word is "elapses", but we understood the suggestion).



$$\left\{ \begin{array}{l} \rho \frac{\partial \omega_i}{\partial t} = \nabla \cdot (\rho D_i \nabla \omega_i + \rho \frac{\omega_i}{M} D_i \nabla M) \\ \omega_3 = 1 - (\omega_1 + \omega_2) \\ @t = 0 \quad \forall x \in \Omega \quad \omega_i = \omega_{i0} \\ @x \in \Gamma_1 \quad \forall t > 0 \quad J_i = 0 \\ @x \in \Gamma_2 \quad \forall t > 0 \quad J_i = 0 \\ @x \in \Gamma_3 \quad \forall t > 0 \quad \omega_i = \omega_{i,eq} \\ @x \in \Gamma_4 \quad \forall t > 0 \quad \omega_i = \omega_{i,eq} \end{array} \right.$$

Controlled drug release from hydrogel-based matrices: experiments and modeling

Diego CACCAVO¹, Sara CASCONE¹, Gaetano LAMBERTI^{1*}, Anna Angela BARBA²

¹ Department of Industrial Engineering, ² Department of Pharmacy,
Via Giovanni Paolo II, 134; University of Salerno; 84084 Fisciano (SA), Italy

* Phone +39 089964077, Fax +39 089964057, E-mail: glamberti@unisa.it

Abstract

Controlled release by oral administration is mainly achieved by pharmaceuticals based on hydrogels. Once swallowed, a matrix made of hydrogels experiences water up-take, swelling, drug dissolution and diffusion, polymer erosion. The detailed understanding and quantification of such a complex behavior is a mandatory prerequisite to the design of novel pharmaceuticals for controlled oral delivery. In this work, the behavior of hydrogel-based matrices has been investigated by means of several experimental techniques previously pointed out (gravimetric, and based on texture analysis); and then all the observed features were mathematically described using a physical model, defined and recently improved by our research group (based on balance equations, rate equations and swelling predictions). The agreement between the huge set of experimental data and the detailed calculations by the model is good, confirming the validity of both the experimental and the theoretical approaches.

Keywords

Hydrogels, Water uptake, Texture analysis, Transport phenomena, Modeling.

Chemical compounds

HydroxyPropyl-MethylCellulose - HPMC (PubChem CID: 57503849); Theophylline (PubChem CID: 2153)

24 Nomenclature

A	Infinitesimal surface [m^2]	\mathbf{v}	Mass average velocity [m/s]
D_i	Pseudo-diffusion coefficient [m^2/s]	\mathbf{v}_{er}	Erosion velocity [m/s]
$D_{i,eq}$	Effective diffusion coefficient of the i^{th} species in the fully swollen matrix [m^2/s]	\mathbf{v}_{swe}	Swelling velocity [m/s]
dr	Radial displacement [m]	Z	Reference axial coordinate of the mesh/material frame [m]
dz	Axial displacement [m]	z	Axial coordinate of the spatial frame [m]
$H(r)$	Tablet semi-thickness, function of the radial position, during the dissolution process [m]	z_0	Initial tablet semi-thickness [m]
\mathbf{J}_i	Diffusive mass flux of the i^{th} species [$kg/(m^2 s)$]	β_i	Fujita-type equation concentration dependence parameter of the i^{th} species [—]
k_{er}	Erosion constant [m/s]	Γ_i	i^{th} boundaries [m]
M	Average molar mass $\left(\left(\sum \frac{\omega_i}{M_i} \right)^{-1} \right)$ [g/mol]	ρ	System density [kg/m^3]
M_i	Molar mass of the i^{th} species [g/mol]	ρ_i	Density of the i^{th} species [kg/m^3]
R	Reference radial coordinate of the mesh/material frame [m]	Ω	Computational domain [m^2]
r	Radial coordinate of the spatial frame [m]	ω_i	Mass fraction of the i^{th} species [—]
r_0	Initial tablet radius [m]	$\omega_{i,0}$	Initial mass fraction of the i^{th} species [—]
r_i	Source term of the i^{th} species [$kg/(m^3 s)$]	$\omega_{i,eq}$	Equilibrium mass fraction of the i^{th} species [—]
t	Time [s]	$\langle \omega_i \rangle(r)$	Average mass fraction on the axial direction function of the radial position [—]

25

26 **1. Introduction**

27 Hydrogels are widely used in the pharmaceutical preparations and, among them, the HydroxyPropyl
28 MethylCellulose (HPMC) is the most extensively appreciated due to its physical, chemical, and biological
29 properties (Phadtare et al., 2014). In fact, this polymer plays a key role in solid and liquid preparations,
30 sustained and controlled release formulations, capsule production, gel and bio-adhesive preparations
31 (Huichao et al., 2014). For the administration of pharmaceuticals, the oral route has been and probably will
32 continue to be the most exploited one thanks to the high patients compliance. The development of
33 controlled release devices suitable for this application has seen in the hydrogel-based tablets the best
34 option to the purpose. These systems benefit from their simplicity of production, low development costs
35 and their highly adaptability in delivering different active molecules.

36 The drug release from HPMC tablets is a complex process, which has been the topic of extensive research in
37 the past few decades. If an hydrogel-based tablet enters in contact with a solvent, which penetrates inside
38 the matrix, the polymer undergoes a relaxation process, due to the unfolding of the polymeric chains. A
39 glass-rubbery transition occurs and a gel-like layer is formed (Grassi et al., 2007). In this region, the
40 elongated chains allow the dissolved drug to easily diffuse and reach the dissolution medium. Once the
41 polymer network have been completely hydrated and the chains disentanglement takes place, the matrix
42 starts to erode. For hydrophilic polymer-based systems, swelling and erosion are the most important
43 mechanisms and, while the swelling implies an increase of the matrix volume, the erosion causes a volume
44 decrease, thus the time dependence of matrix volume is determined by the combined and opposing action
45 of these two phenomena (Grassi and Grassi, 2014). Concerning the drug release from hydrophilic matrices,
46 it can be influenced by several factors, which depend on the drug (such as its molecular weight, solubility,
47 particle size distribution, and the initial dose), on the polymer used (such as its molecular weight,
48 composition, structure, and viscosity) (Tahara et al., 1995), on formulation (such as the geometry of the
49 matrix, excipients presence, and manufactory process) (Sung et al., 1996), on external factors (such as the
50 dissolution medium composition, ionic strength, and temperature) (Maderuelo et al., 2011; Zuleger and
51 Lippold, 2001). Thus, it is clear the difficulty of a full understanding and characterization of all the
52 phenomena involved in the drug release from these systems.

53 During the last decades, several approaches have been used to describe the behavior of these systems,
54 from both the experimental and the modeling point of view. To study the swelling behavior of a matrix,
55 theoretical considerations are usually the starting points useful to define the release mechanism (i.e.
56 assessment of swelling controlled release mechanism based on the use of dimensionless analysis (Ferrero
57 et al., 2010), use of thermodynamic parameters of activation to discriminate between diffusion and
58 relaxation control for the solvent penetration (Ferrero et al., 2013), evaluation of the self-diffusion of the
59 solute and of the water in hydrogels to explain deviations from Fickian diffusion (Ferrero et al., 2008)). To
60 evaluate the water uptake into a tablet, different experimental methods have been proposed in literature,
61 ranging from weighing the swollen and the dried matrix (Mamani et al., 2012) to NMR microscopy (Rajabi-
62 Siahboomi et al., 1994). Swelling progression and mobility of water molecule inside polymers have been
63 investigated by several technologies, including magnetic resonance imaging (MRI) (Kikuchi et al., 2012),
64 atomic force microscopy (AFM), texture analyzer, ultrasound techniques (Huanbutta et al., 2013). To
65 quantify the swelling phenomena, a rheological analysis to measure the evolution of viscoelastic behavior
66 of the gel layer as it swells using an oscillatory indentation (Hewlett et al., 2012), the use of a stereoscopic
67 microscope (Choi et al., 2014), an optical image analysis (Gao and Meury, 1996; Gao et al., 1996) have been
68 proposed. To measure the matrix erosion and the consequent polymer dissolution, a phenol-sulphuric acid
69 technique using a spectrometric analysis can be applied (Ghori et al., 2014). Moreover, a combination of
70 determination of the expansion factor, texture analysis, visual swelling observation of dye containing

71 tablets, and photomicroscopy used together allows the investigation of dimensional changes, swelling
72 velocity, thickness, appearance and strength of the gel layer and front movements (Zuleger et al., 2002). To
73 evaluate the drug, polymer, and water amount residual in a matrix after a certain dissolution time, a
74 combination of gravimetric and image analysis techniques can be used (Barba et al., 2009a; Barba et al.,
75 2009b; Chirico et al., 2007).

76 Recently, the texture analysis as approach to pharmaceutical research and development has been
77 extensively used (Li and Gu, 2007; Li et al., 2008). In general, from a compression experiment a force-time
78 diagram is obtained and the hardness of the system, the work of cohesion (the work necessary to
79 overcome the internal bonds of the material), and the work of adhesion (the work necessary to pull the
80 probe away from the swollen tablet) can be evaluated (Conti et al., 2007). Using this device the correlation
81 between drug dissolution and polymer hydration from a modified release matrix can be obtained,
82 measuring the work necessary to penetrate the swollen matrix after a certain dissolution time and
83 correlating it to the water uptake (Jamzad et al., 2005; Lamberti et al., 2013). The simultaneous
84 measurements of the dimensional changes in the swollen gel and in the glassy core during the dissolution
85 of a matrix can be achieved using a texture analyzer equipped with a special probe (Nazzal et al., 2007).

86 Due to the complexity of the phenomena involved during the hydration of hydrogel-based matrices, in the
87 study and in the development of these systems the use of mathematical modeling can be of great aid.
88 Several modeling approaches have been proposed in literature during the years, starting from the semi-
89 empirical model of Higuchi (Higuchi, 1961), where a square root dependence of drug release from time (for
90 a thin film geometry) was found, later generalized by Peppas and his coworkers (Peppas, 1984), until the
91 recent approach followed by (Caccavo et al., 2015), where a model based on the transport equations
92 coupled with a deforming domain through the ALE (Arbitrary Lagrangian Eulerian) method has been
93 proposed. The release rate from hydrophilic matrices can be described using simplified approaches, i.e.
94 considering that diffusion is the sole mechanism of drug release (ignoring the swelling mechanism) (Gao et
95 al., 1995), considering that determined system specific model parameters (such as apparent drug diffusion
96 coefficients in the polymeric matrix) can be biased using simplified theories (Siepmann et al., 2013).
97 Increasing the complexity a 3D model, taking into account both the drug release from a swelling hydrogel-
98 based matrix and the erosion phenomenon was proposed (Siepmann et al., 1999a; Siepmann and Peppas,
99 2000; Siepmann et al., 1999b). The major drawback of this model was the hypothesis of affine
100 deformations, therefore the initial cylindrical shape is maintained during the dissolution process and the
101 matrix volume increase as the water penetrate into the system. These limiting hypotheses were later
102 removed considering that the inlet water flux is the driven force for the swelling (Lamberti et al., 2011). In
103 this model, the polymer mass was derived from a macroscopic balance and the unconstrained mass
104 fractions could lead to some local unrealistic results. This inaccuracy was overcome coupling the polymer
105 mass description with the mass transport equations for drug and water by the use of mass fraction
106 constraints (Kaunisto et al., 2010; Kaunisto et al., 2013).

107 **1.1 Aim of the work**

108 The aim of this work is then to make use of the recently proposed model (Caccavo et al., 2015) to describe
109 all the phenomena which take place during the complex process of hydrogel-based matrices hydration, by
110 comparison with the very large set of experimental data gathered by several experimental techniques,
111 including the detailed water content distribution obtained by texture analysis (Cascone et al., 2014).

112

113 2. Materials and Methods

114 2.1 Materials

115 Powders of HydroxyPropyl-MethylCellulose (HPMC, Methocel K15M, kindly supplied by Colorcon, Varese,
116 Italy) and theophylline (TP, CAS number 58-55-9, Sigma Aldrich, Milan, Italy) have been used to produce the
117 matrices. Deionized water, HCl (37% w/w, Sigma–Aldrich, CAS number 7647-01-0) and sodium phosphate
118 tribasic dodecahydrate (Sigma–Aldrich, CAS number 10101-89-0) have been used for the dissolution media
119 preparation.

120 2.2 Matrices preparation

121 HPMC and TP powders have been mixed (TP/HPMC 50% wt/wt) and compressed using a cylindrical
122 tableting machine (Specac PN3000, equipped with flat-faced punches), applying a loading force of 50 kN,
123 kept for 5 min by a press. For the ‘radial dissolution’ tests, the matrices dimensions are: radius 6.5 mm,
124 thickness 2 mm, weight 350 ± 5 mg; for the ‘semi-overall dissolution’ tests: radius 6.5 mm, thickness 1 mm,
125 weight 175 ± 2 mg.

126 2.3 Dissolution methods

127 To reproduce the matrix behavior after its administration, different media have been used to reproduce the
128 gastrointestinal environments during the dissolution tests. In fact, a pharmaceutical form is firstly ingested
129 from the mouth and arrives into the stomach, where it finds an acidic environment. To reproduce this
130 condition, the dissolution medium in this first phase has been kept at pH 1 preparing a solution containing
131 6.25 mL of HCl diluted with deionized water to 750 mL for two hours, the average physiological residence
132 time in the stomach. To simulate the passage into the intestinal environment, which is almost neutral, the
133 dissolution medium has been neutralized adding 250 mL of deionized water containing 19 gr of sodium
134 phosphate tribasic dodecahydrate. The medium during all the tests has been kept at 37°C and at constant
135 rotation speed of 100 rpm in a USP II apparatus (AT7Smart, Sotax, Allschwil, Switzerland). The dissolutions
136 have been performed under the same conditions for all the tests.

137 Two different dissolution tests have been performed on the matrices, the first type, the ‘radial dissolution’
138 has been performed on matrices confined between two glass slides to ensure only the lateral uptake of
139 water. Using this method, the matrix swells only in radial direction and preserves its thickness. Once the
140 matrix has been withdrawn from the dissolution medium, the superior slide has been removed and the
141 matrix has been subjected to the gravimetric or mechanical analysis. References for further details (Barba
142 et al., 2009a; Barba et al., 2009b). The second type of dissolution experiments, the ‘semi-overall
143 dissolution’ tests, has been performed on matrices glued in a small center-part on a glass slab paying
144 attention to overlap the centers of the tablet and of the glass slab. The matrix is free to swell both in axial
145 and in radial direction, and the glass slide could be seen as the symmetry plane orthogonal to the z-axis
146 (the cylinder axis) of a tablet with a thickness twice the one used in this test.

147 2.4 Gravimetric, optical, and mechanical methods

148 The gravimetric method has been used to evaluate the mass amounts of the three components (polymer,
149 drug, and water) in the swollen matrix according to a previously developed technique (Barba et al., 2009a).
150 This technique has been applied only for the radial dissolution and the water content measured has been
151 used as calibration to obtain the relation between water content and force-penetration diagram obtained
152 from the mechanical tests, as described in (Cascione et al., 2014). At given immersion times, the sample has
153 been withdrawn and the superior slide has been removed. Then, the swollen matrix has been cut by several
154 thin-walled metallic punch, and each portion has been recovered and quantitatively transferred on a glass
155 holder. The cutting procedures have been repeated by using punches of decreasing radius, obtaining

156 several annuli and a central core, which have been placed on different glass holder. All the samples have
157 been dried till reaching a constant weight to obtain the amount of water in each section. Then, the dried
158 tablet sections have been completely dissolved, to allow the determination of the drug content and thus
159 the determination of the polymer fraction. These operations have been repeated for all the dissolution
160 time considered (for radial dissolution: 24, 48, 72, and 96 hours), obtaining the evolutions of mass fractions
161 with both the time and the radial direction. All the runs were performed in triplicate, and results have been
162 showed as average values, with their proper standard deviation.

163 With reference to the semi-overall dissolution, only the total mass amounts of the components after the
164 hydration (for semi-overall dissolution: 2, 3, 4, 6, 8, and 24 hours) have been evaluated. To evaluate the
165 water up-take of the matrix, it has been weighted, dried, and then weighted again, the water mass entered
166 in the matrix during the dissolution can be thus evaluated, from the difference between the two weights.
167 The dried matrix has been completely dissolved, to determine the drug content by the use of the High
168 Performance Liquid Chromatography (HPLC) method described in the next section. The residual polymer
169 mass has been obtained knowing the total weight after the hydration and the drug and water masses.
170 Repeating these analyses for several hydration times, the drug, the polymer and the water masses
171 evolution inside the tablet, as functions of the hydration time, have been obtained.

172 To evaluate the swollen matrix size, an image analysis technique has been applied. Once withdrawn from
173 the dissolution medium, the matrix has been carefully removed and an overhead photo has been taken.
174 From this image the diameter of the matrix after erosion and swelling phenomena has been measured. To
175 measure the thickness and evaluate the shape of the hydrated matrix, after each dissolution time, the
176 matrix has been carefully cut along a diameter and photographed from the side. **From these pictures, both
177 the swollen gel layer and the glassy core are clearly visible.**

178 The drug release, for both the radial and the semi-overall dissolution methods has been evaluated
179 **withdrawing** a sample of the medium after the dissolution and analyzing it according to the analytical
180 method described in the next section.

181 The mechanical tests have been performed according to a previously described procedure (Cascone et al.,
182 2014). Indentation tests using a texture analyzer (TA.XT Plus Stable Micro System Godalming, UK equipped
183 with a needle probe and a 5 kg loading cell) have been performed on swollen matrices for both the radial
184 and semi-overall systems. Matrices have been penetrated axially at several distances from the center. The
185 indentation test velocity has been kept constant at 0.03 mm/s, the instrument measuring the force
186 necessary to penetrate into the swollen matrix. Data acquisition starts when the probe touches the sample
187 (i.e. where the sample offers a not negligible force to penetration) and it ends when the probe reaches the
188 90% of the total sample thickness with a recording rate of 100 points/s. To ensure reproducibility of the
189 data, every test has been performed in triplicate and results have been shown as average values.

190 **2.5 Analytical methods**

191 In the present work, the analytical determinations to evaluate the amount of theophylline in solution have
192 been performed using an Agilent 1200 Infinity Series HPLC (Agilent Technologies, Milano, Italy). The
193 analyses have been performed using a C-18 column (Nucleodur 100-5 ec C18, by MACHEREY-NAGEL)
194 equipped with a column guard and the detection has been performed at 275 nm wavelength. The flow rate
195 of the eluent phase has been set on 2 mL/min of a solution composed by acetonitrile and acid acetic/water
196 0.2% vol solution, according with the gradient elution described in Table 1. **The large number of samples to
197 be assayed has led to choose the use of HPLC over the faster UV-Vis method because of the availability of
198 the automatized auto-sampler, which allowed to run a large number of testing overnight.**

199 3. Modeling

200 The dissolution process has been virtualized using the model proposed by (Caccavo et al., 2015) where the
201 whole matrix release behavior is described using mass transport equations, to describe the species
202 diffusion, coupled with the ALE (Arbitrary Lagrangian Eulerian) method, to consider the system swelling.

203 The computational domains in this work have been a quarter and half of the whole tablet, respectively for
204 the radial and the semi-overall dissolutions, represented by a rectangle in the 2D-axial symmetric
205 configuration (Figure 1).

206 The transport equations employed, with the proper initial and boundary conditions, have been the same as
207 in (Caccavo et al., 2015), for water (i=1) and drug (i=2), while the polymer (i=3) has been derived from the
208 mass fraction constraint:

$$\begin{array}{cc}
 \text{Radial} & \text{Semi-overall} \\
 \left\{ \begin{array}{l} \rho \frac{\partial \omega_i}{\partial t} = \nabla \cdot (\rho D_i \nabla \omega_i + \rho \frac{\omega_i}{M} D_i \nabla M) \\ \omega_3 = 1 - (\omega_1 + \omega_2) \\ @t = 0 \forall \mathbf{x} \in \Omega \omega_i = \omega_{i0} \\ @x \in \Gamma 1 \forall t > 0 \mathbf{J}_i = 0 \\ @x \in \Gamma 2 \forall t > 0 \mathbf{J}_i = 0 \\ @x \in \Gamma 3 \forall t > 0 \mathbf{J}_i = 0 \\ @x \in \Gamma 4 \forall t > 0 \omega_i = \omega_{i,eq} \end{array} \right. & \left\{ \begin{array}{l} \rho \frac{\partial \omega_i}{\partial t} = \nabla \cdot (\rho D_i \nabla \omega_i + \rho \frac{\omega_i}{M} D_i \nabla M) \\ \omega_3 = 1 - (\omega_1 + \omega_2) \\ @t = 0 \forall \mathbf{x} \in \Omega \omega_i = \omega_{i0} \\ @x \in \Gamma 1 \forall t > 0 \mathbf{J}_i = 0 \\ @x \in \Gamma 2 \forall t > 0 \mathbf{J}_i = 0 \\ @x \in \Gamma 3 \forall t > 0 \omega_i = \omega_{i,eq} \\ @x \in \Gamma 4 \forall t > 0 \omega_i = \omega_{i,eq} \end{array} \right. \quad (1)
 \end{array}$$

209 In particular, in the mass fluxes the Fick's first law for dilute systems, where the driving force is the molar
210 fraction, has been translated for concentrate systems, where the driving force is the mass fraction. In this
211 derivation the molar mass terms arise (Caccavo et al., 2015).

212 With the constitutive equations described by the following equation for the diffusivities:

$$D_i = D_{i,eq} \exp \left[-\beta_i \left(1 - \frac{\omega_i}{\omega_{1,eq}} \right) \right] \quad (2)$$

213 and an ideal mixing rule for the specific volume for the system density:

$$\frac{1}{\rho} = \left(\sum \frac{\omega_i}{\rho_i} \right) \quad (3)$$

214 The domain deformation has been modeled considering that the domain is freely deformable and the
215 deformation is driven by the movements of the boundaries Γ_i , accordingly to Laplace smoothing equations
216 (Caccavo et al., 2015; COMSOL, 2013):

$$\begin{array}{cc}
 \text{Radial} & \text{Semi-overall} \\
 \left\{ \begin{array}{l} \frac{\partial^2}{\partial R^2} \left(\frac{\partial r}{\partial t} \right) + \frac{\partial^2}{\partial Z^2} \left(\frac{\partial r}{\partial t} \right) = 0 \\ \frac{\partial^2}{\partial R^2} \left(\frac{\partial z}{\partial t} \right) + \frac{\partial^2}{\partial Z^2} \left(\frac{\partial z}{\partial t} \right) = 0 \\ @t = 0 \quad r = r_0; z = z_0 \\ @x \in \Gamma 1 \forall t > 0 \quad dr = 0, dz = 0 \\ @x \in \Gamma 2 \forall t > 0 \quad dz = 0 \\ @x \in \Gamma 3 \forall t > 0 \quad dz = 0 \\ @x \in \Gamma 4 \forall t > 0 \quad \frac{\partial r}{\partial t} = (\mathbf{v}_{swe} + \mathbf{v}_{er})|_r \end{array} \right. & \left\{ \begin{array}{l} \frac{\partial^2}{\partial R^2} \left(\frac{\partial r}{\partial t} \right) + \frac{\partial^2}{\partial Z^2} \left(\frac{\partial r}{\partial t} \right) = 0 \\ \frac{\partial^2}{\partial R^2} \left(\frac{\partial z}{\partial t} \right) + \frac{\partial^2}{\partial Z^2} \left(\frac{\partial z}{\partial t} \right) = 0 \\ @t = 0 \quad r = r_0; z = z_0 \\ @x \in \Gamma 1 \forall t > 0 \quad dr = 0 \\ @x \in \Gamma 2 \forall t > 0 \quad dz = 0 \\ @x \in \Gamma 3 \forall t > 0 \quad \frac{\partial z}{\partial t} = (\mathbf{v}_{swe} + \mathbf{v}_{er})|_z \\ @x \in \Gamma 4 \forall t > 0 \quad \frac{\partial r}{\partial t} = (\mathbf{v}_{swe} + \mathbf{v}_{er})|_r \end{array} \right. \quad (4)
 \end{array}$$

217 The free-boundaries (Γ_4 for radial case, Γ_3 and Γ_4 for semi-overall case) move with a velocity due to swelling
218 and erosion; the other boundaries describe physical constraints: for radial case Γ_1 is a symmetry axis,

219 whereas Γ_2 and Γ_3 are planes which don't allow vertical translations; for semi-overall case Γ_1 is a symmetry
220 axis and Γ_2 is a plane which doesn't allow vertical translations.

221 The swelling velocity can be computed from a flow identity at interface, as shown by (Caccavo et al., 2015):

$$v_{swe} = -\frac{(J_1 + J_2)}{\rho \omega_3} \quad (5)$$

222 whereas the erosion velocity is accounted as a constant value (fitting parameter):

$$|v_{er}| = -k_{er} \quad (6)$$

223 3.1 Code solving

224 The previous Partial Differential Equations (PDEs) have been solved with the Finite Element Methods (FEM)
225 using the commercial software COMSOL Multiphysics® 4.3b. The development and implementation of the
226 simulations have been carried out with the help of a workstation based on the processor Intel® Core™ i7-
227 4820K with a clock rate of 3.70 GHz and a RAM of 64 GB. The computational domain was divided in 725 and
228 385 quadrilateral elements (with dimensions between 8.25×10^{-7} and 2.44×10^{-4} m) for the semi-overall
229 and the radial simulation, respectively, with particular high elements density close to the erosion
230 boundaries. The results obtained are mesh-size independent and the calculation time have been 19 min for
231 the semi-overall simulations and 37 s for the radial simulations.

232 4. Results and discussion

233 4.1 Radial dissolution

234 In the radial dissolution tests, the matrices behavior has been monitored for 4 days, gathering experimental
235 data each 24 h. In Figure 2 the total mass evolution of each component inside the swollen matrix is shown.
236 The drug release is particularly slow in this configuration, where the surface through which the system can
237 exchange matter is only the lateral one, reaching at maximum the 60% of theophylline release in 4 days.
238 However the release rate is higher in the first 24 h, sensibly decreasing after that time. This can be
239 explained considering that in this configuration within the first day the drug close to the tablet lateral
240 surface is promptly released whereas after this first part the presence of a gel layer increasing in thickness
241 takes over and the drug transport and its release become more and more difficult, leading to a decrease of
242 the release rate. On the other hand even the polymer dissolution is very limited, particularly in the first
243 48 hours, bringing to a final dissolution of about 20% of the initial polymer amount in the matrix. The water
244 uptake considerably increases in the first 3 days, slowing down after that time. The curves in Figure 2
245 represent the modeling results obtained using the model proposed by (Caccavo et al., 2015). Most of the
246 parameters (Table 2) have been applied as they were in the original model whereas the water Fujita-type
247 equation coefficient (β_1) has been modified using the data by Gao et al. (Gao and Fagerness, 1995) and the
248 drug effective diffusion coefficient ($D_{2,eq}$) has been slightly increased to better describe the drug release.
249 The erosion constant has been used as fitting parameter as in the original model.

250 With this minimum parameters adjustment the model results seem to describe nicely all the “macroscopic”
251 experimental results (Figure 2).

252 The so tuned model has been compared to microscopic experimental results. In Figure 3 the data from the
253 gravimetric and the texture analyses allow to completely characterize the system in terms of components
254 distribution inside the swollen tablets. The horizontal bars represent the radius of the tablet parts (annulus
255 or core) analyzed, therefore the experimental point is an average value of the part examined. The texture
256 data represent local water mass fraction that is uniform along the tablet height (Lamberti et al., 2013). As it

257 can be seen these two techniques are in good agreement and give precise information on the hydration of
258 the swollen tablet. The other gravimetric data, on drug and polymer mass fractions, allow to close the mass
259 balances on the whole system. After 24 h (Figure 3/a) the tablet core is almost not hydrated and as the
260 dissolution time **elapses** the inner part of the tablet get more and more hydrated, reaching the 50% wt/wt
261 after 96 h (Figure 3/d) in the tablet core. The drug mass fraction profiles instead highlight the phenomenon
262 of the faster drug release rate in the first 24 h with respect to greater dissolution times. Indeed the drug
263 mass fraction close to the erosion front (Figure 3/a) shows the depletion of drug inside the swollen tablet
264 for several millimeters, confirming the promptly dissolution and release of the theophylline close to the
265 erosion front, whereas in the tablet core its mass fraction is still the original one. After the initial
266 dissolution/release behavior, the inner tablet parts play the role of a drug storage, allowing its gradual
267 release along with the tablet hydration (Figure 3/b-d). The polymer distribution, besides confirming the
268 equilibrium polymer mass fraction at the erosion front (3% wt/wt), shows the gradual polymer dilution
269 along with the tablet swelling.

270 The modeling results have been compared to the experimental results using the mass fraction profiles
271 along the tablet radius (at any height) that, in this system, is equal to the $\langle\omega_i\rangle(t, r)$ (Caccavo et al., 2015) since
272 the mass fraction is constant along the axial direction. The modeling water mass fraction profiles in the first
273 48 h (Figure 3/a-b) slightly underestimate the experimental points whereas, at the same times, there is an
274 overestimation in the macroscopic water uptake. This is explainable considering that a greater swollen
275 tablet radius is predicted, and in the external layers the amount of water is predominant (97% of the total
276 mass), bringing to an overestimation of the macroscopic water adsorption, despite the underestimation of
277 the internal mass fraction profiles. However, the experimental mass fraction profiles are satisfactorily well
278 described, since no further parameters adjustment is requested at this stage (zero parameter model)
279 (Figure 3).

280 4.2 Semi-overall dissolution

281 The same HPMC-theophylline system has been used for “semi-overall” dissolution analyses. These tests, as
282 described in the ‘Materials and Methods’ section, have been set up to reproduce the behavior of the
283 overall dissolution tests exploiting the disc planar symmetry. Indeed half amount of components has been
284 utilized to form tablets, with respect to the normal tablets (e.g. the tablets employed for the radial tests),
285 and the lower tablet part has been centrally glued on a glass slab to reproduce the symmetry condition of
286 the overall system: the null mass flux. In this way the system behavior can be characterized in terms of
287 macroscopic data (e.g. residual masses and shape) and in terms of microscopic data (e.g. hydration via
288 texture analyses). In the semi-overall dissolution tests the tablets behavior has been analyzed for 24 h. In
289 Figure 4/a are reported the residual masses inside the swollen matrices as well as the percentage of drug
290 release.

291 In this configuration the surfaces through which the system can exchange matter are the lateral and the top
292 part, substantially changing the release behavior with respect to the radial experiments. Indeed, after 24 h
293 of dissolution the drug release is close to the 97% (just the 38% in the radial tests) and the water uptake is
294 close to 1 g (less than 0.4 g in the radial tests whereas in an overall experiment it should be 2 g). The
295 polymer dissolution/release, like in the radial experiments, is very limited in the dissolution time analyzed.
296 In Figure 4/b the erosion radius and thickness obtained from the photos are shown, taking the maximum
297 radius and the central height (at $r=0$). As it can be seen, the axial swelling is quite pronounced, increasing of
298 almost 6 times with respect to the initial thickness, whereas the radial expansion is somewhat less evident,
299 despite the increment is of 1.5 times the initial radius. The model tuned on the macroscopic radial
300 experiments has been applied with the same parameters, apart the erosion constant, (Table 2) to the semi-

301 overall configuration, changing the boundary conditions as shown in the 'Modeling' section. As it can be
302 seen all the experimental results in Figure 4/a-b are well predicted by the model, allowing the complete
303 characterization of the macroscopic behavior of the tablet dissolution in the semi-overall configuration.

304 In order to fully investigate the matrix behavior, the swollen matrices have been subjected to texture
305 analyses to obtain the hydration level. The technique gives information on the water content along the
306 axial distance: repeating the analysis at several radii it is possible to build a contour plot that shows the
307 hydration level in the whole swollen tablet. As explained in Cascone et al. (Cascone et al., 2014) this type of
308 analysis is not able to detect the presence of the fully swollen layer ($\omega_1 > 0.9$) due to its low resistance to the
309 needle penetration. However these simple analyses give detailed information on the internal water content
310 that can be compared with pictures of the swollen tablet as well as with modeling results. In Figure 5
311 swollen tablet pictures (top left part) with texture analysis results (top right part), and modeling water mass
312 fraction distribution (bottom right part) at several dissolution times (2, 3, 6 and 8 h) are shown.

313 Both the texture and the modeling data are expressed in terms of water mass fraction content, starting
314 from zero (black) in the dry regions up to more than 0.9 in the fully swollen regions (light gray). From these
315 graphs it is possible to see that the internal tablet hydration level, as well as the final swollen tablet shape,
316 are well predicted by the model thanks to the comparison with the texture analysis results and the swollen
317 matrix pictures, respectively. This confirms, once again, the validity of the model proposed by Caccavo et al.
318 (Caccavo et al., 2015), that is able to predict in a satisfactorily manner all the phenomena involved in a
319 tablet dissolution process, as well as the effectiveness of the experimental methods employed in the
320 characterization of the swollen tablets.

321 5. Conclusions

322 Hydrogels are extensively used in pharmaceutical preparations due to their peculiar behavior. In this work
323 the main transport phenomena which take place when an hydrogel-based matrix loaded with a soluble
324 drug is subjected to dissolution tests have been analyzed, both by experimental and modeling approaches.
325 Two different systems have been studied, the first one, a simplified system which allows only the radial
326 uptake of water, has been characterized in term of polymer and drug release and water uptake, together
327 with the determination of all the three components along the swollen matrix radius. The mass amounts
328 into the matrix have been measured using a gravimetric technique, moreover, a texture analysis has been
329 performed to determine the water uptake along the matrix height at several radii during the dissolution.
330 The second system analyzed, the semi-overall one, which allows the water uptake both in radial and axial
331 directions, besides being analyzed in terms of polymer and drug release and water uptake, has been
332 subjected to an image analysis to measure the dimensions (radius and height) of the swollen matrices after
333 several dissolution times and to a mechanical analysis to determine the water content inside the matrix. A
334 mathematical model previously proposed (Caccavo et al., 2015), based on the combined use of the mass
335 transport equations and the ALE method to describe the diffusion of the species in the matrix during the
336 dissolution and the swelling phenomenon, has been adapted to describe these systems. In particular,
337 although most of the model parameters used have been derived from the original model, the water Fujita-
338 type equation coefficient and the drug effective diffusion coefficient have been slightly modified and the
339 erosion constant has been used as fitting parameter on the basis of the best fitting of macroscopic
340 experimental results. The model, tuned by comparison with macroscopic experimental data (drug, polymer
341 and water masses evolution with time), was found able to satisfactorily describe the matrix size and shape
342 during the hydration. Furthermore, the availability of a recently pointed out technique for water content
343 measurement (Cascone et al., 2014), allowed to compare the model calculations with the experimental
344 info.

345 Therefore and in conclusion, in this work two tools have been successfully used to investigate the behavior
346 of hydrogel based matrices: an easy and fast experimental technique based on texture analysis to evaluate
347 the water content (Cascone et al., 2014); and a powerful and detailed model able to describe all the
348 phenomena which take place during the hydration of the matrices (Caccavo et al., 2015). These tools can
349 be of great aid for designing and testing new hydrogel-based pharmaceutical systems.

350 **Acknowledgements**

351 This work was supported by the Ministero dell'Istruzione dell'Università e della Ricerca (contract grant
352 PRIN 2010-11 – 20109PLMH2).

353 **Conflicts of interest**

354 The authors confirm that there are no known conflicts of interest associated with this publication and there
355 has been no significant financial support for this work that could have influenced its outcome.

356

357 **References**

- 358 Barba, A.A., D'Amore, M., Cascone, S., Chirico, S., Lamberti, G., Titomanlio, G., 2009a. On the behavior of
359 HPMC/theophylline matrices for controlled drug delivery. *J Pharm Sci-U* 98, 4100-4110.
- 360 Barba, A.A., d'Amore, M., Chirico, S., Lamberti, G., Titomanlio, G., 2009b. Swelling of cellulose derivative
361 (HPMC) matrix systems for drug delivery. *Carbohyd Polym* 78, 469-474.
- 362 Caccavo, D., Cascone, S., Lamberti, G., Barba, A.A., 2015. Modeling the drug release from hydrogel-based
363 matrices. *Mol Pharm* 12, 474-483.
- 364 Cascone, S., Lamberti, G., Titomanlio, G., d'Amore, M., Barba, A.A., 2014. Measurements of non-uniform
365 water content in hydroxypropyl-methyl-cellulose based matrices via texture analysis. *Carbohyd Polym* 103,
366 348-354.
- 367 Chirico, S., Dalmoro, A., Lamberti, G., Russo, G., Titomanlio, G., 2007. Analysis and modeling of swelling and
368 erosion behavior for pure HPMC tablet. *J Control Release* 122, 181-188.
- 369 Choi, D.H., Lim, J.Y., Shin, S., Choi, W.J., Jeong, S.H., Lee, S., 2014. A Novel Experimental Design Method to
370 Optimize Hydrophilic Matrix Formulations with Drug Release Profiles and Mechanical Properties. *J Pharm*
371 *Sci-U* 103, 3083-3094.
- 372 COMSOL, 2013. Chapter 18. Deformed Geometry and Moving Mesh, COMSOL Multiphysics Reference
373 Manual VERSION 4.3b.
- 374 Conti, S., Maggi, L., Segale, L., Ochoa Machiste, E., Conte, U., Grenier, P., Vergnault, G., 2007. Matrices
375 containing NaCMC and HPMC: 1. Dissolution performance characterization. *Int J Pharmaceut* 333, 136-142.
- 376 Ferrero, C., Massuelle, D., Doelker, E., 2010. Towards elucidation of the drug release mechanism from
377 compressed hydrophilic matrices made of cellulose ethers. II. Evaluation of a possible swelling-controlled
378 drug release mechanism using dimensionless analysis. *J Control Release* 141, 223-233.
- 379 Ferrero, C., Massuelle, D., Jeannerat, D., Doelker, E., 2008. Towards elucidation of the drug release
380 mechanism from compressed hydrophilic matrices made of cellulose ethers. I. Pulse-field-gradient spin-
381 echo NMR study of sodium salicylate diffusivity in swollen hydrogels with respect to polymer matrix
382 physical structure. *J Control Release* 128, 71-79.
- 383 Ferrero, C., Massuelle, D., Jeannerat, D., Doelker, E., 2013. Towards elucidation of the drug release
384 mechanism from compressed hydrophilic matrices made of cellulose ethers. III. Critical use of
385 thermodynamic parameters of activation for modeling the water penetration and drug release processes. *J*
386 *Control Release* 170, 175-182.
- 387 Gao, P., Fagerness, P.E., 1995. Diffusion in HPMC gels. I. Determination of drug and water diffusivity by
388 pulsed-field-gradient spin-echo NMR. *Pharmaceutical research* 12, 955-964.
- 389 Gao, P., Meury, R.H., 1996. Swelling of hydroxypropyl methylcellulose matrix tablets. 1. Characterization of
390 swelling using a novel optical imaging method. *J Pharm Sci-U* 85, 725-731.
- 391 Gao, P., Nixon, P.R., Skoug, J.W., 1995. Diffusion in HPMC gels. II. Prediction of drug release rates from
392 hydrophilic matrix extended-release dosage forms. *Pharmaceutical research* 12, 965-971.
- 393 Gao, P., Skoug, J.W., Nixon, P.R., Robert Ju, T., Stemm, N.L., Sung, K.C., 1996. Swelling of hydroxypropyl
394 methylcellulose matrix tablets. 2. Mechanistic study of the influence of formulation variables on matrix
395 performance and drug release. *J Pharm Sci-U* 85, 732-740.
- 396 Ghori, M.U., Ginting, G., Smith, A.M., Conway, B.R., 2014. Simultaneous quantification of drug release and
397 erosion from hypromellose hydrophilic matrices. *Int J Pharmaceut* 465, 405-412.
- 398 Grassi, M., Grassi, G., 2014. Application of mathematical modeling in sustained release delivery systems.
399 *Expert opinion on drug delivery* 11, 1299-1321.
- 400 Grassi, M., Grassi, G., Lapasin, R., Colombo, I., 2007. Understanding Drug Release and Absorption
401 Mechanisms: A Physical and Mathematical Approach. Taylor & Francis.
- 402 Hewlett, K.O., L'Hote-Gaston, J., Radler, M., Shull, K.R., 2012. Direct measurement of the time-dependent
403 mechanical response of HPMC and PEO compacts during swelling. *Int J Pharmaceut* 434, 494-501.
- 404 Higuchi, T., 1961. Rate of release of medicaments from ointment bases containing drugs in suspension.
405 *Journal of pharmaceutical sciences* 50, 874-875.
- 406 Huanbutta, K., Terada, K., Sriamornsak, P., Nunthanid, J., 2013. Advanced technologies for assessment of
407 polymer swelling and erosion behaviors in pharmaceutical aspect. *Eur J Pharm Biopharm* 83, 315-321.

- 408 Huichao, W., Shouying, D., Yang, L., Ying, L., Di, W., 2014. The application of biomedical polymer material
409 hydroxy propyl methyl cellulose (HPMC) in pharmaceutical preparations. *Journal of Chemical and*
410 *Pharmaceutical Research* 6, 155-160.
- 411 Jamzad, S., Tutunji, L., Fassihi, R., 2005. Analysis of macromolecular changes and drug release from
412 hydrophilic matrix systems. *Int J Pharmaceut* 292, 75-85.
- 413 Kaunisto, E., Abrahmsen-Alami, S., Borgquist, P., Larsson, A., Nilsson, B., Axelsson, A., 2010. A mechanistic
414 modelling approach to polymer dissolution using magnetic resonance microimaging. *J Control Release* 147,
415 232-241.
- 416 Kaunisto, E., Tajarobi, F., Abrahmsen-Alami, S., Larsson, A., Nilsson, B., Axelsson, A., 2013. Mechanistic
417 modelling of drug release from a polymer matrix using magnetic resonance microimaging. *European*
418 *Journal of Pharmaceutical Sciences* 48, 698-708.
- 419 Kikuchi, S., Onuki, Y., Kuribayashi, H., Takayama, K., 2012. Relationship between diffusivity of water
420 molecules inside hydrating tablets and their drug release behavior elucidated by magnetic resonance
421 imaging. *Chemical and Pharmaceutical Bulletin* 60, 536-542.
- 422 Lamberti, G., Cascone, S., Cafaro, M.M., Titomanlio, G., d'Amore, M., Barba, A.A., 2013. Measurements of
423 water content in hydroxypropyl-methyl-cellulose based hydrogels via texture analysis. *Carbohydrate*
424 *polymers* 92, 765-768.
- 425 Lamberti, G., Galdi, I., Barba, A.A., 2011. Controlled release from hydrogel-based solid matrices. A model
426 accounting for water up-take, swelling and erosion. *International journal of pharmaceutics* 407, 78-86.
- 427 Li, H., Gu, X., 2007. Correlation between drug dissolution and polymer hydration: a study using texture
428 analysis. *Int J Pharmaceut* 342, 18-25.
- 429 Li, H., Hardy, R.J., Gu, X., 2008. Effect of drug solubility on polymer hydration and drug dissolution from
430 polyethylene oxide (PEO) matrix tablets. *Aaps Pharmscitech* 9, 437-443.
- 431 Maderuelo, C., Zarzuelo, A., Lanao, J.M., 2011. Critical factors in the release of drugs from sustained release
432 hydrophilic matrices. *J Control Release* 154, 2-19.
- 433 Mamani, P.L., Ruiz-Caro, R., Veiga, M.D., 2012. Matrix Tablets: The Effect of Hydroxypropyl
434 Methylcellulose/Anhydrous Dibasic Calcium Phosphate Ratio on the Release Rate of a Water-Soluble Drug
435 Through the Gastrointestinal Tract I. *In Vitro Tests. Aaps Pharmscitech* 13, 1073-1083.
- 436 Nazzal, S., Nazzal, M., El-Malah, Y., 2007. A novel texture-probe for the simultaneous and real-time
437 measurement of swelling and erosion rates of matrix tablets. *Int J Pharmaceut* 330, 195-198.
- 438 Peppas, N., 1984. Analysis of Fickian and non-Fickian drug release from polymers. *Pharmaceutica acta*
439 *Helveticae* 60, 110-111.
- 440 Phadtare, D., Ganesh Phadtare, N.B., Asawat, M., 2014. Hypromellose—A Choice of Polymer in Extended
441 Release Tablet Formulation. *World Journal of Pharmacy and Pharmaceutical Sciences* 3, 551-566.
- 442 Rajabi-Siahboomi, A., Bowtell, R., Mansfield, P., Henderson, A., Davies, M., Melia, C., 1994. Structure and
443 behaviour in hydrophilic matrix sustained release dosage forms: 2. NMR-imaging studies of dimensional
444 changes in the gel layer and core of HPMC tablets undergoing hydration. *J Control Release* 31, 121-128.
- 445 Siepmann, J., Karrou, Y., Gehrke, M., Penz, F., Siepmann, F., 2013. Predicting drug release from
446 HPMC/lactose tablets. *Int J Pharmaceut* 441, 826-834.
- 447 Siepmann, J., Kranz, H., Bodmeier, R., Peppas, N., 1999a. HPMC-matrices for controlled drug delivery: a new
448 model combining diffusion, swelling, and dissolution mechanisms and predicting the release kinetics.
449 *Pharmaceutical research* 16, 1748-1756.
- 450 Siepmann, J., Peppas, N., 2000. Hydrophilic matrices for controlled drug delivery: an improved
451 mathematical model to predict the resulting drug release kinetics (the "sequential layer" model).
452 *Pharmaceutical research* 17, 1290-1298.
- 453 Siepmann, J., Podual, K., Sriwongjanya, M., Peppas, N., Bodmeier, R., 1999b. A new model describing the
454 swelling and drug release kinetics from hydroxypropyl methylcellulose tablets. *Journal of pharmaceutical*
455 *sciences* 88, 65-72.
- 456 Sung, K., Nixon, P.R., Skoug, J.W., Ju, T.R., Gao, P., Topp, E., Patel, M., 1996. Effect of formulation variables
457 on drug and polymer release from HPMC-based matrix tablets. *Int J Pharmaceut* 142, 53-60.
- 458 Tahara, K., Yamamoto, K., Nishihata, T., 1995. Overall mechanism behind matrix sustained release (SR)
459 tablets prepared with hydroxypropyl methylcellulose 2910. *J Control Release* 35, 59-66.

- 460 Zuleger, S., Fassihi, R., Lippold, B.C., 2002. Polymer particle erosion controlling drug release. II. Swelling
461 investigations to clarify the release mechanism. *Int J Pharmaceut* 247, 23-37.
462 Zuleger, S., Lippold, B.C., 2001. Polymer particle erosion controlling drug release. I. Factors influencing drug
463 release and characterization of the release mechanism. *Int J Pharmaceut* 217, 139-152.
464

465 **Tables and figures**

466 No table of figures entries found.

467

468

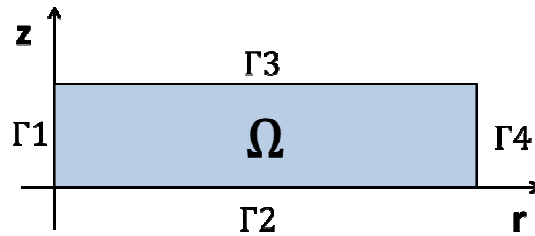
469 **Table 1. Parameters of HPLC analysis.**

Gradient elution	Time	Acetonitrile - Acetic acid/water 0.2% vol.
	min	Composition
	0	3%-97%
	6	4%-96%
	12	6%-94%
Flow rate	2 mL/min	
Injection volume	5 μ L	
Temperature	25°C	
Elution time	15 min	

470

471 **Table 2. Values of the parameters used in the simulations.**

<i>From experiments/literature</i>		
r_0	Initial tablet radius [mm]	6.5
z_0	Initial tablet semi-thickness (radial) or thickness (semi-overall) [mm]	1
ω_{10}	Initial water mass fraction [–]	0
ω_{20}	Initial drug mass fraction [–]	0.5
ω_{30}	Initial polymer mass fraction [–]	0.5
ρ_1	Water density [kg/m ³]	1000
ρ_2	Drug density [kg/m ³]	1200
ρ_3	Polymer density [kg/m ³]	1200
M_1	Water molecular weight [g/mol]	18
M_2	Drug molecular weight [g/mol]	180.16
M_3	Polymer molecular weight [g/mol]	120000
<i>From experiments/hypotheses</i>		
$\omega_{1,eq}$	Equilibrium water mass fraction [–]	0.97
$\omega_{2,eq}$	Equilibrium drug mass fraction [–]	0
<i>From literature/optimization</i>		
$D_{1,eq}$	Water effective diffusivity in the fully swollen matrix [m ² /s]	2.2×10^{-9}
$D_{2,eq}$	Drug effective diffusivity in the fully swollen matrix [m ² /s]	1.5×10^{-10}
β_1	Water Fujita-type equation coefficient [–]	3.53 (Gao and Fagerness, 1995)
β_2	Drug Fujita-type equation coefficient [–]	4
k_{er} (radial)	Erosion constant [m/s]	10×10^{-9} (fitting)
k_{er} (semi-overall)	Erosion constant [m/s]	5×10^{-9} (fitting)



472

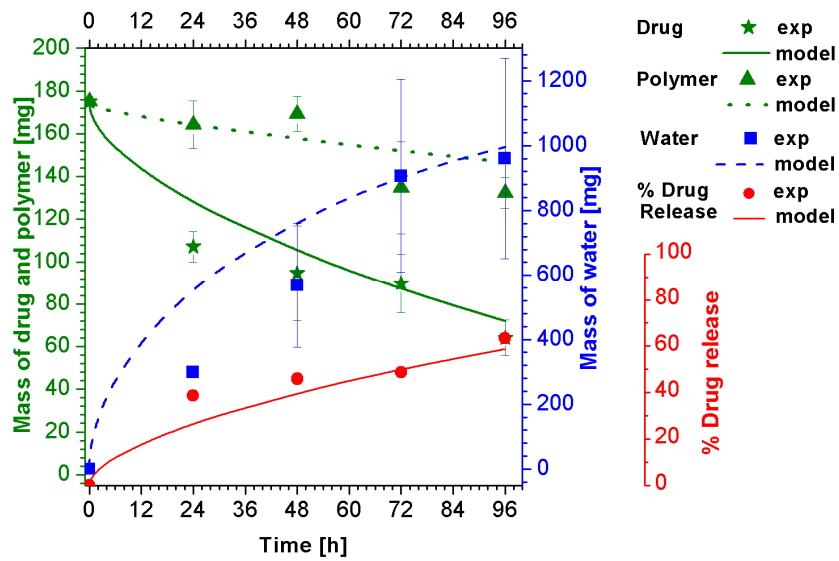
473

474

475

476

Figure 1. Computational domain representing a quarter of the whole tablet in the radial tests and half tablet in the semi-overall test. The physical meaning of the domain boundaries is the following. Radial tests: Γ_1 =axial symmetry, Γ_2 =plane of symmetry, Γ_3 =in contact with the glass slab, Γ_4 =erosion boundary. Semi-overall tests: Γ_1 =axial symmetry, Γ_2 =centrally glued (0,0) on the glass slab, Γ_3 =erosion boundary, Γ_4 =erosion boundary.



477

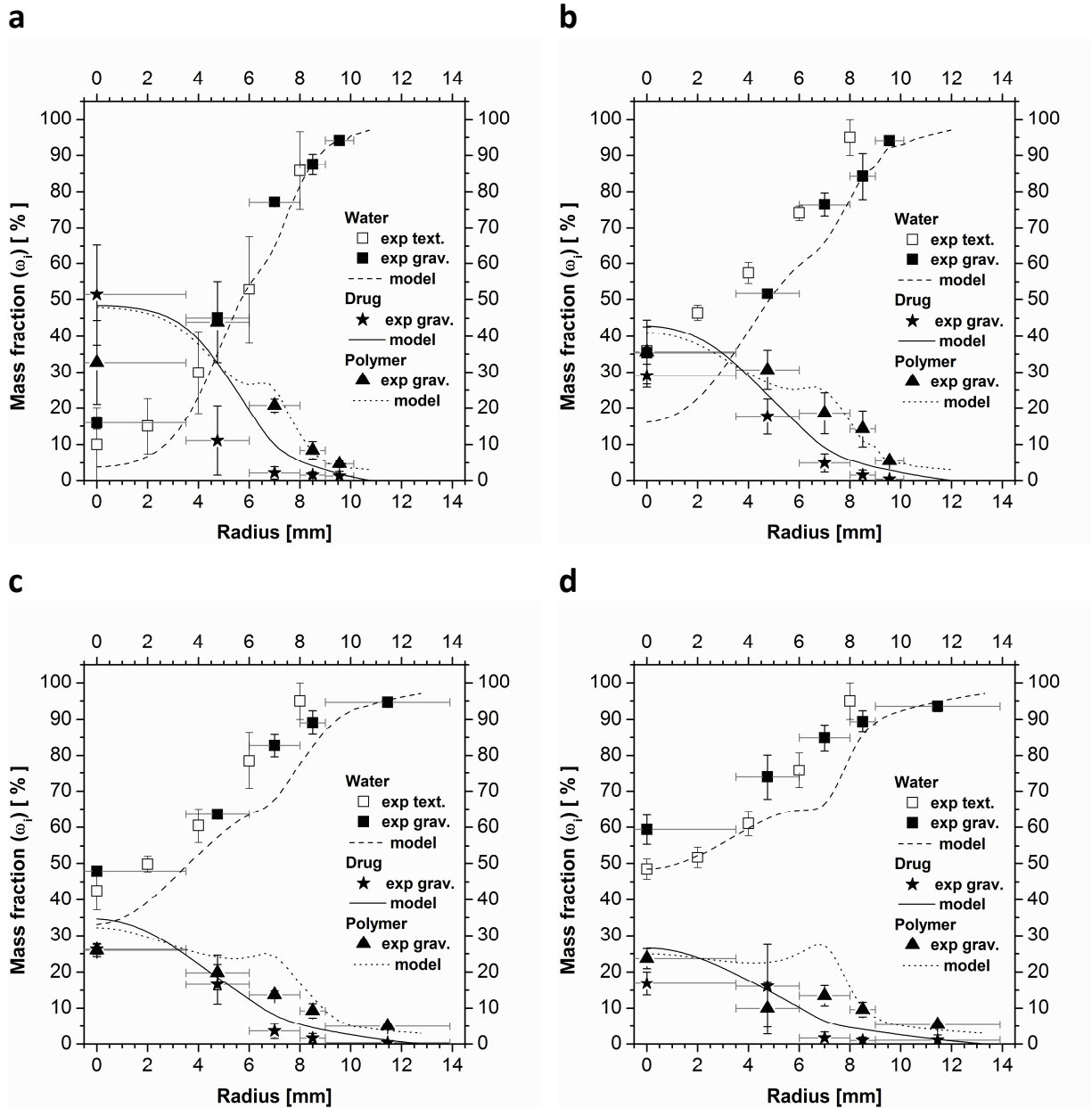
478

479

480

Figure 2. Radial dissolution: mass of drug, polymer (green) and water (blue) inside the swollen tablet at different dissolution times. In red the percentage of drug release.

481



482

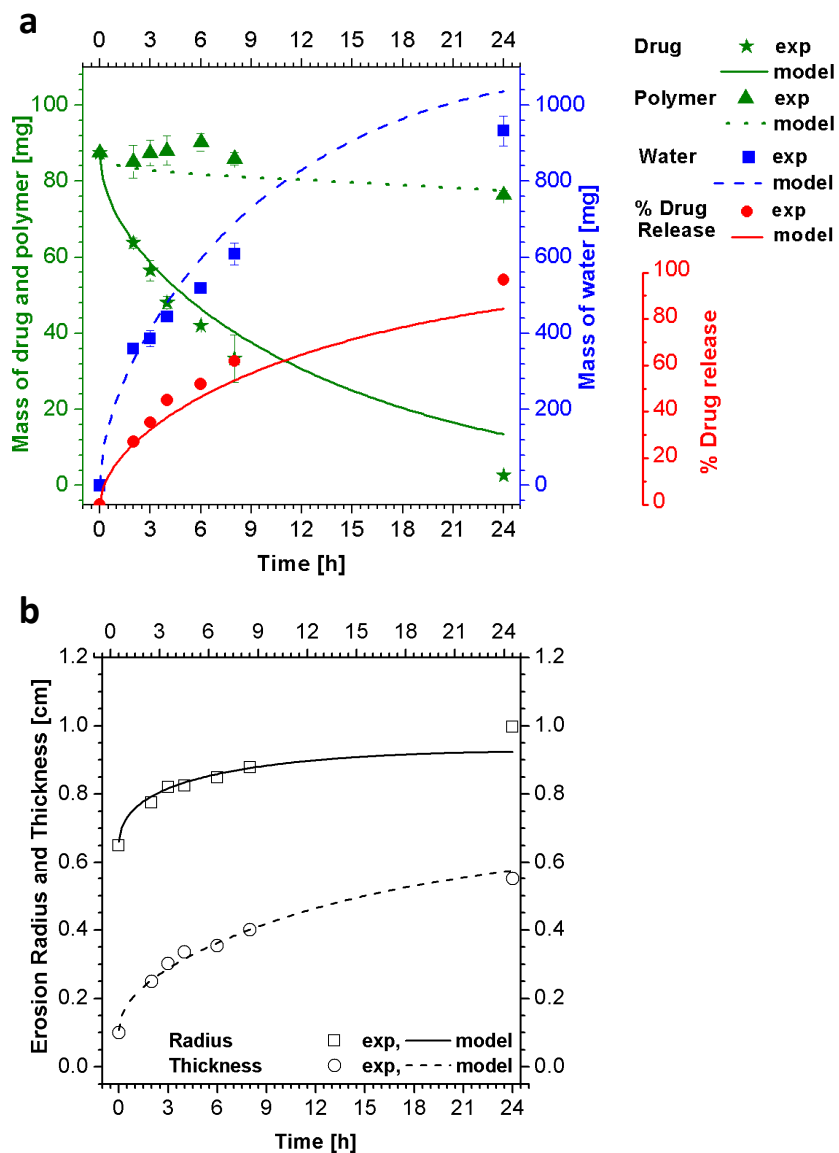
483

484

485

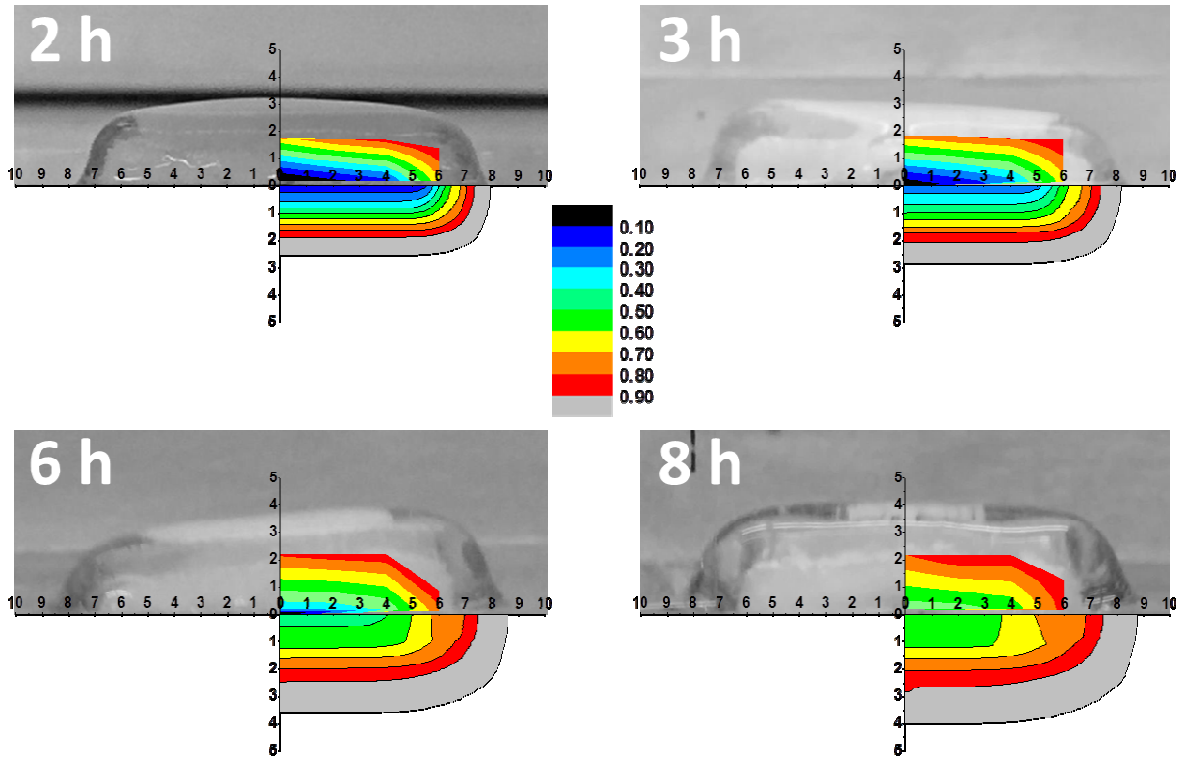
Figure 3. Radial dissolution: comparison between experimental and calculated results in terms of mass profiles along the radial direction. Dissolution times of 24 h (a), 48 h (b), 72 h (c), 96 h (d).

486



487 Figure 4. Semi-overall dissolution: (a) mass of drug, polymer (green) and water (blue) inside the tablet at different dissolution
 488 times. In red the percentage of drug release. (b) Erosion radius and thickness of the swollen tablet.

489



490

491

492

493

494

Figure 5. Semi-overall dissolution: comparison between experimental and modeling results in terms of tablets pictures (top part of the graphs), experimental water mass fraction from texture analysis (top right part of the graphs) and modeling water mass fraction (bottom right part of the graphs). All the spatial dimensions are in mm; color scale is referred to water content mass fraction (black = dry matrix; light gray = fully hydrated matrix).